Title
GERMANIUM DETECTORS WITH A BUILT-IN TRANSVERSE DRIFT FIELD

Authors
Luke, P.N.
Madden, N.W.
Goulding, F.S.

Publication Date
1984-11-01

Lawrence Berkeley Laboratory
UNIVERSITY OF CALIFORNIA

Engineering & Technical Services Division

Presented at the IEEE 1984 Nuclear Science Symposium, Orlando, FL, October 31 - November 2, 1984; and to be published in IEEE Transactions on Nuclear Science

GERMANIUM DETECTORS WITH A BUILT-IN TRANSVERSE DRIFT FIELD

P.N. Luke, N.W. Madden, and F.S. Goulding

November 1984

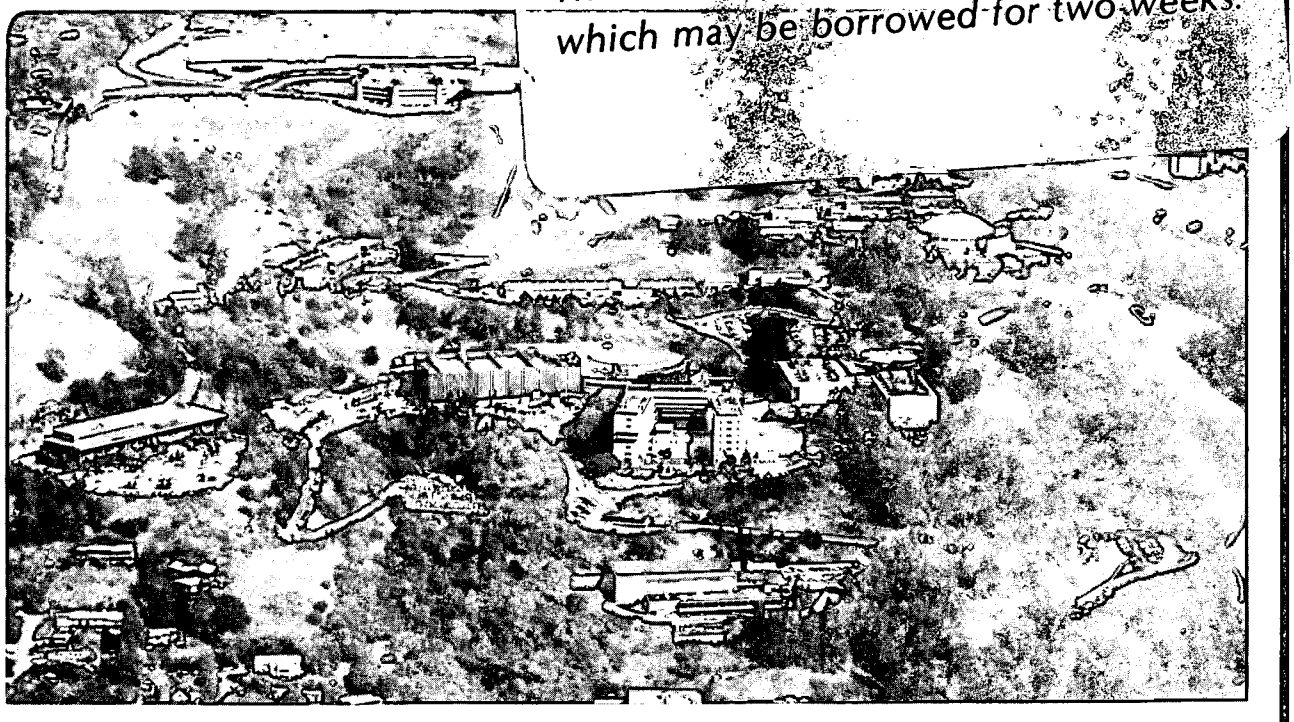

Prepared for the U.S. Department of Energy under Contract DE-AC03-76SF00098

DISCLAIMER

GERMANIUM DETECTORS WITH A BUILT-IN TRANSVERSE DRIFT FIELD

LBL-17780

P. N. Luke, N. W. Madden, F. S. Goulding
Department of Instrument Science and Engineering
Lawrence Berkeley Laboratory
University of California
Berkeley, California 94720 U.S.A.

Abstract

A new kind of position-sensitive germanium detector based on a novel mode of charge transport is proposed and experimental devices have been fabricated. In these germanium "drift-chambers", position information is obtained by measuring carrier drift times. One-dimensional spatial resolutions of $\lesssim 0.5$ mm over an active area of ~ 2.5 x 2.5 cm^2 have been achieved in one detector for 60 keV photons. The simplicity of such detectors makes them attractive as position-sensitive gamma-ray spectrometers compared to discrete element detectors. The problems and limitations of the present detectors are discussed.

Introduction

Recently, Gatti et al. proposed a method of realizing semiconductor "drift chambers" through the use of a novel charge transport mechanism [1,2]. These so-called "drift-chambers" are position-sensitive detectors in which the position information is obtained by measuring drift times of charge carriers traveling in a potential well normal to the initial charge collection. This can greatly reduce the number of readout channels required compared to that of conventional discrete-element semiconductor detectors for the same spatial resolution. Also, in principle, this method potentially improves energy resolution because of the low capacitance exhibited by such detectors in the output circuit. This fact may result in high-resolution photon spectrometers with large active areas.

An idealized structure of the "drift chamber" is shown in Fig. 1a. It has a planar p^+-n-p^+ structure with an n^+ contact along one edge. With the opposing p^+ contacts held at the same potential and reverse bias applied between them and the n^+ contact, depletion of the bulk n-type region starts from both p^+ contacts. Before full depletion, a conducting layer of undepleted material exists at the middle of the detector and the capacitance of the device as measured between the n^+ and the p^+ contacts remains high. As the bias (V) is increased, the undepleted layer shrinks in thickness and the capacitance decreases as $V^{-1/2}$. At full depletion, the conducting layer disappears and the capacitance drops abruptly to a low value which is equal to the geometric capacitance between the n^+ and the two p^+ contacts. For uniform detector thickness and crystal impurity concentration, the potential inside the detector at full depletion is depicted in Fig. 1b. The depth of the potential well (V_W) is just the depletion voltage which is the same as that of a simple planar detector with half the thickness. As carriers are generated in the detector by ionizing radiation, the holes are collected by the p^+ contact while the electrons drift toward the middle of the detector (Fig. 1b). In order to collect the electrons, a transverse drift field (i.e. parallel to the detector plane) is needed. The scheme for accomplishing this as originally proposed by Gatti and Rehak [1] is to tilt the whole potential distribution by segmenting the p^+ contacts into strips and applying a linearly graded potential to them. Prototype silicon detectors with such a configuration has been fabricated and preliminary test results published [2]. However, this scheme requires segmenting the contacts on both sides of the wafer and connecting each segment to an external potential. This creates difficulties in the fabrication and use of such detectors. This paper reports on a different method of obtaining the transverse drift field without contact segmentations and the test results of germanium detectors fabricated based on this concept. Germanium was chosen because of the availability of the special material required and the promise of producing simple position-sensitive gamma-ray and high energy x-ray detectors with good energy resolution.

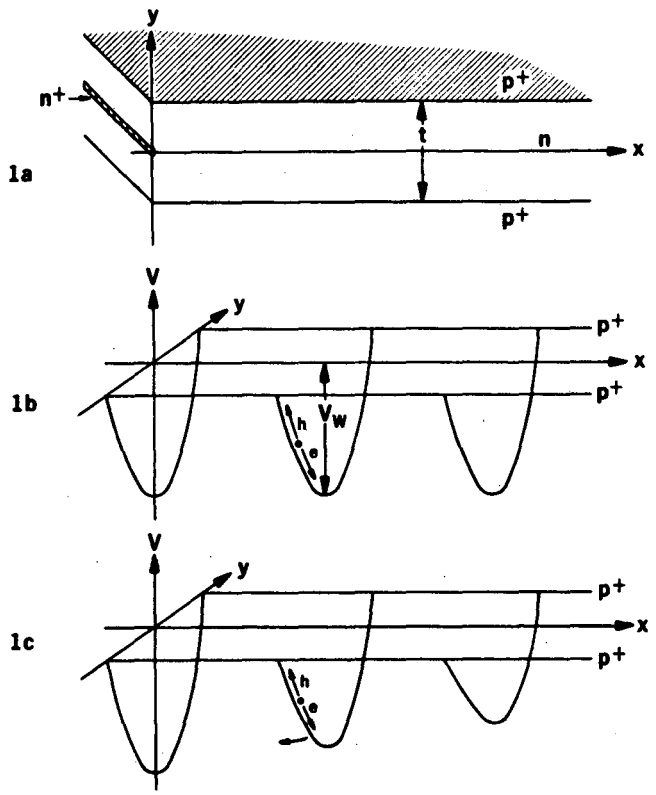

XBL 8410-4071

Fig. 1. Idealized structure of the semiconductor "drift chamber" (a), and the resulting potential distributions at full depletion for (b) uniform impurity concentration, and (c) for material with an impurity concentration gradient.

Principle of Operation

A transverse drift field without the need of contact segmentation or externally applied potential gradient can be achieved by using material with an impurity concentration gradient along the detector plane. For a detector with an increasing impurity concentration towards the n^+ contact, depletion at the far end of the detector will occur at a lower bias resulting in a shallower potential well (V_W). Depletion occurs at increasingly higher bias as one approaches the n^+ contact, creating a potential distribution at full depletion shown in Fig. 1c. The built-in transverse drift field thus obtained at the midplane of the detector is given by:

$$E_{drift} = \frac{dV_w(x)}{dx} = \frac{t^2 e}{8\epsilon} \cdot \frac{dN(x)}{dx}$$

where t is the detector thickness, N(x) is the impurity concentration, e is the electronic charge, and ϵ is the permittivity. Note that in order to obtain a constant transverse drift field, a linear impurity gradient is required.

While a suitable bulk impurity gradient in detector-grade silicon crystals may be difficult to obtain, high-purity germanium crystals routinely grown for nuclear radiation detectors often exhibit an increasing net n-type impurity concentration toward the tail due to the segregation of phosphorus impurities during crystal growth [3]. Slices taken from a suitable section and cut parallel to the growth axis can be used to fabricate the detectors. Besides the concentration gradient, the absolute concentration is also important as it determines the magnitude of the electric field perpendicular to the p^+ contacts. The average value of this field should be much higher than the transverse drift field so as to improve the timing characteristics and decrease uncertainties in the measurement of carrier drift times.

The structure and approximate dimensions of the detectors that were fabricated are shown in Fig. 2. They were chosen mainly for the relative ease of fabrication and handling, and because they represent appropriate dimensions that might be used in actual applications. A transverse drift field of ~ 50 Vcm^{-1} was aimed for, which will give a reasonable drift time for the electrons of ~ 0.5 $\mu sec\ cm^{-1}$.

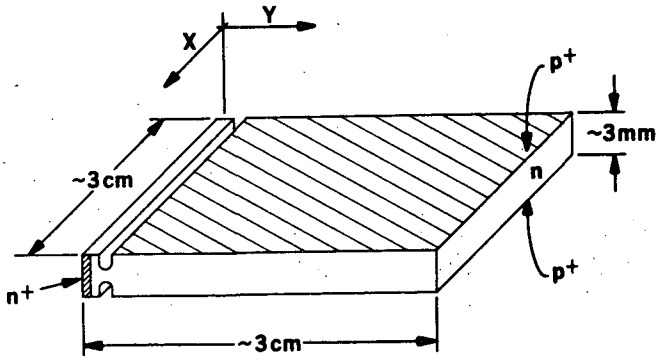

Fig. 2. Structure and approximate dimensions of the detectors.

Figure 3 describes schematically the development of signals at the three contacts due to charges deposited in the upper half of the detector by, for example, a photoelectric event. As the electrons (-Q) and holes (+Q) separate and travel perpendicular to the detector plane, currents are induced at both p^+ contacts. This is similar to that of a simple planar detector. However, since the charges travel only half the detector thickness, a total charge of 1/2 Q is induced at each p^+ contact. The polarity of the signal is opposite for the two p^+ contacts and it depends on which half of the detector the interaction occurs. As the electrons drift horizontally, virtually no signal is induced until the charge packet comes into close proximity to the n^+ contact [1]. As the electrons are collected, a charge of +1/2 Q is induced at each p^+ contact and a charge of -Q is induced at the n^+ contact. As can be seen, unique start and stop timing signals needed for determining carrier drift times are obtained from the separate contacts. The availability of prompt signals from the detector is an important feature because otherwise position determination for random, uncorrelated photons would not be possible. Because the prompt signals induced at the two p^+ contacts are opposite in polarity, they will cancel out unless separate signal channels are provided. Also, for the same reason, radiations that produce an equal amount of ionizations in the two halves of the detector will not generate any signal even with separate channels. (However, this may not be true if the two p^+ contacts are maintained at different potentials so that the potential well minima is shifted toward one p^+ contact). This is the case for high-energy charged-particles but, in this case, a prompt signal can be easily obtained using an additional detector.

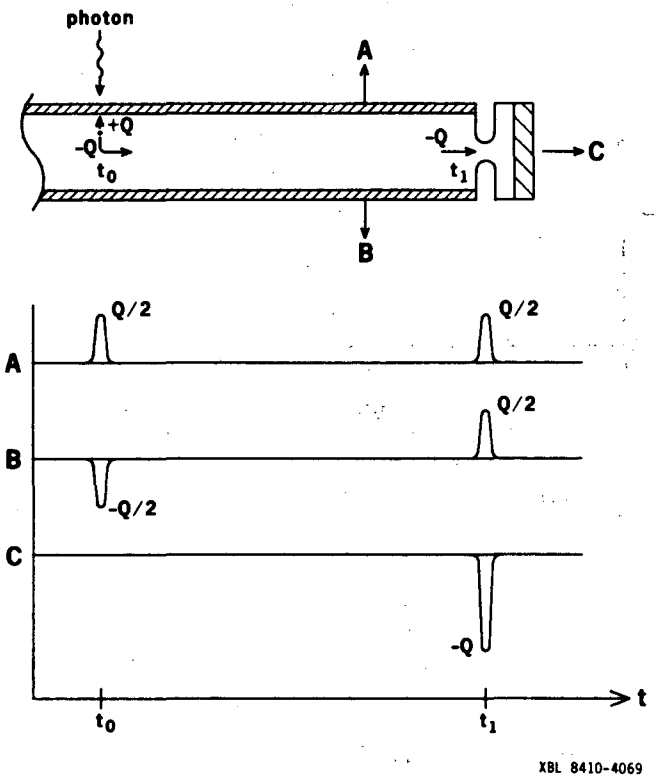

Fig. 3. Development of signals due to charge deposited in the upper half of the detector.

Test Results

Experimental detectors were fabricated from sections taken from two different crystals numbered 649 and 603. The detectors are designated as 649-14a and 603-14a respectively. The structure and approximate dimensions are as shown in Fig. 2. The n^+ contacts are formed by lithium diffusion while the p^+ contacts are formed by boron ion implantation.

The capacitance-voltage characteristics of the two detectors are shown in Fig. 4. They show the expected drastic drop in the capacitance as the detectors are being depleted. The drop in capacitance is not as abrupt as in the case of uniform impurity concentration, but the capacitance at full depletion has the same low value. The positions on the curves where the capacitances begin to decrease rapidly correspond to the depletion of the far end of the detectors while the positions where they begin to flatten correspond to full depletion. From this, the impurity concentrations of the two detectors were estimated to be approximately $6 \times 10^{10} cm^{-3}$ to $1.2 \times 10^{11}\ cm^{-3}$ for detector 649-14a and $8 \times 10^{10} cm^{-3}$ to $2.5 \times 10^{11} cm^{-3}$ for detector 603-14a, and corresponding average transverse drift fields of ~ 30 Vcm^{-1} and ~ 60 Vcm^{-1}, respectively.

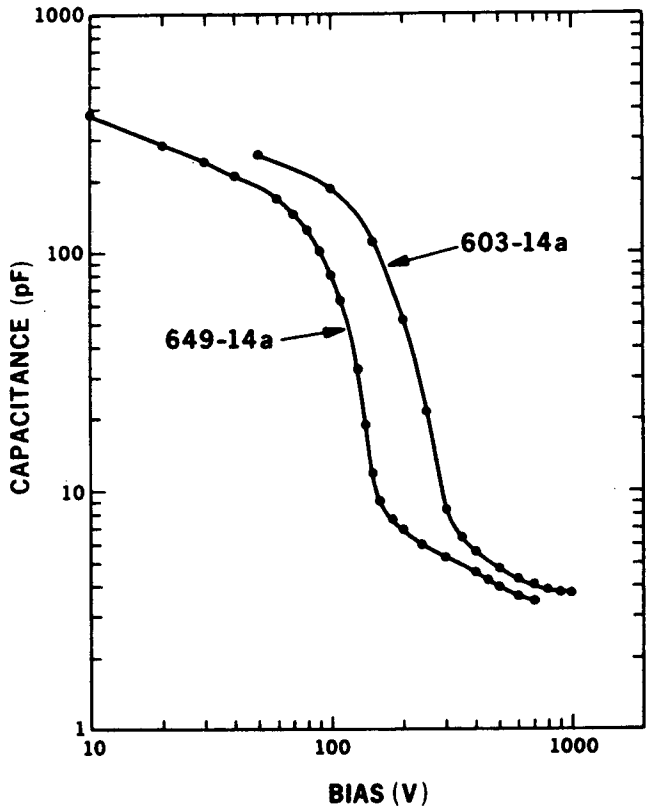

Fig. 4. Capacitance-voltage characteristics of the detectors.

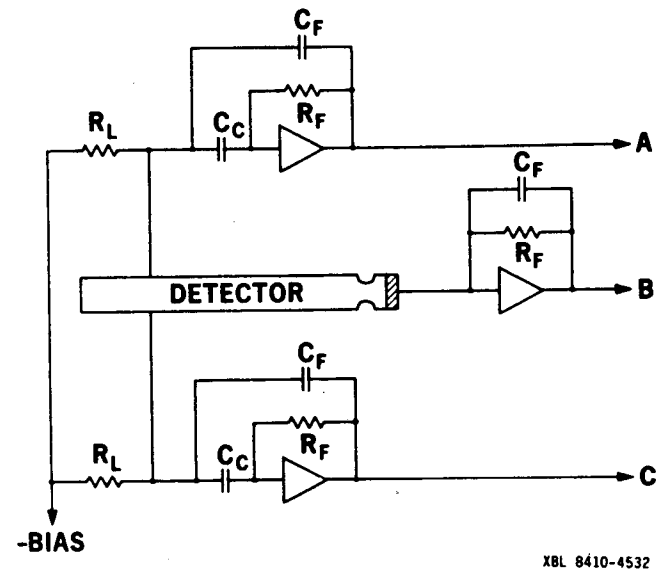

Fig. 5. Configuration of electronics used in evaluating the detectors.

The electronic configuration used to evaluate the detectors is shown in Fig. 5. The FET input stage of the preamplifiers and the components shown are mounted near the detector inside a cryostat. The two separate AC-coupled preamplifiers connected to the p^+ contacts provide the "start" timing signals for drift time measurements while the DC coupled amplifier at the n^+ contact, which "sees" the small detector capacitance, gives the "stop" timing signal and the energy information. The contiguous p^+ contact greatly simplifies the connection of the amplifiers to them, compared to the original scheme with segmented contacts. The feedback capacitors (C_F) of the AC-coupled preamplifiers are connected as shown to reduce charge division effects associated with the series connected coupling capacitor (C_C). The detectors were scanned using a collimated ^{241}Am, 60 keV gamma-ray source with an approximately 0.5 mm diameter spot size located outside the cryostat's vacuum enclosure. Scans were made parallel to the X and Y axis as defined in Fig. 2.

Figure 6 displays the actual wide-band signals obtained from the three preamplifiers arising from 60 keV gamma-rays interacting near the far end and in the upper half of the detector. The negative going signals from channel C and that from channel B were used to trigger a time-to-amplitude converter and the resulting signals stored in a pulse-height analyzer. Coincidence with the condition that a signal corresponding to ~ 60 keV is obtained at channel B is also used to cut down the rate of chance triggerings due to noise spikes and background radiations.

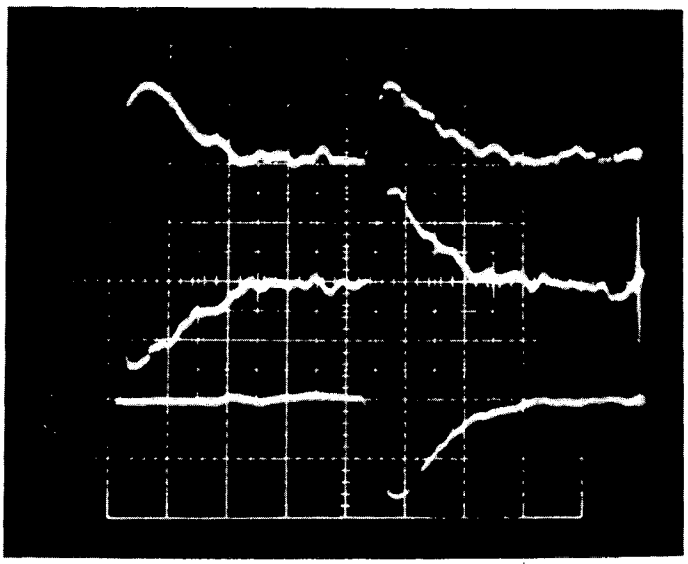

XBB 840-8175

Fig. 6. Oscilloscope traces of wide-band signals from, starting at the top, channels A, C and B respectively as indicated in Fig. 5. All three traces are triggered by the negative going signals from channel C. The horizontal scale is 500 ns per division.

The time spectrum of a scan parallel to the Y axis of detector 649-14a at increments of 2 mm is shown in Fig. 7. The average FWHM of the peaks is about 50 nsec corresponding to about 0.5 mm which is comparable to the contribution expected from the spot size of the collimated source. This implies a spatial resolution better than 0.5 mm for 60 keV gamma rays. The drift times versus the actual source positions are plotted in Fig. 8. It consists of two very linear sections with slightly differing slopes of 108 nsec mm^{-1} and 85 nsec mm^{-1}. The change in slope occurs at about Y = 15 mm reflecting a change in impurity concentration gradient at that point. This seems to be correlated with the position along the crystal where its diameter begins to increase.

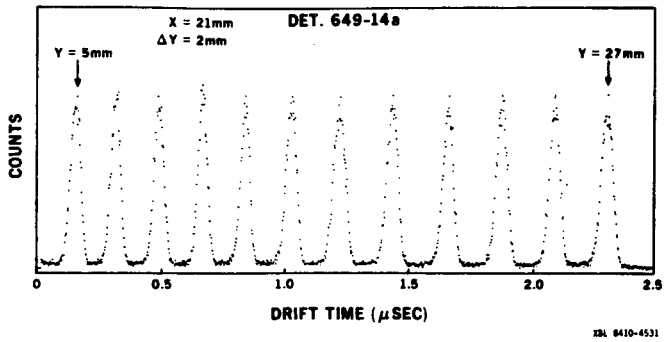

Fig. 7. Time spectrum of a scan along detector 649-14a at increments of 2 mm using a collimated ^{241}Am 60 keV gamma-ray source. Detector bias = 200 V.

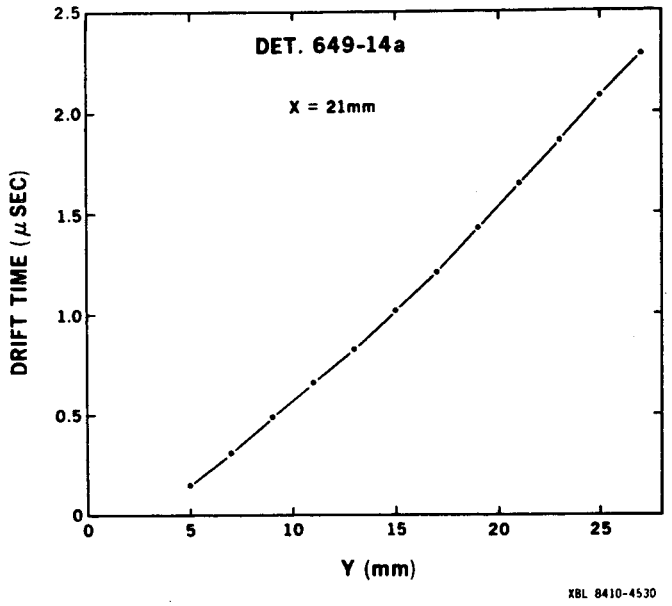

Fig. 8. A plot of drift time versus position with data obtained in Fig. 7.

Figure 9 shows the results of scans made parallel to the X axis at various drift distances. It is seen that up to a drift distance of 17 mm, the drift times are very uniform across the detector with variations in the range of 0.15 mm. At a drift distance of 25 mm, the variation increased to ~ 0.5 mm.

Due to the low drift field and long drift distances of the electrons, the spectral resolution of this kind of detector is expected to be extremely sensitive to the presence of electron traps. ^{241}Am spectra taken by illuminating the whole area of detector 649-14a are shown in Fig. 10. At low temperatures the 60 keV peak is considerably broadened. Spectra taken with a collimated source showed good energy resolution but the pulse heights decrease as one moves away from the n^+ contact due to the increasing probability of electrons being trapped. Thus, the broadened peaks of the full area spectra are the result of the varying degree of trappings along the detector. At higher temperatures, the spectral lines begin to improve, presumably due to the faster release time of electrons from the traps. Above about 135 K, the effect of trappings is in large part eliminated. It is important to point out that due to the strong dependence of carrier mobility on temperature, the carrier drift time at 135 K is about

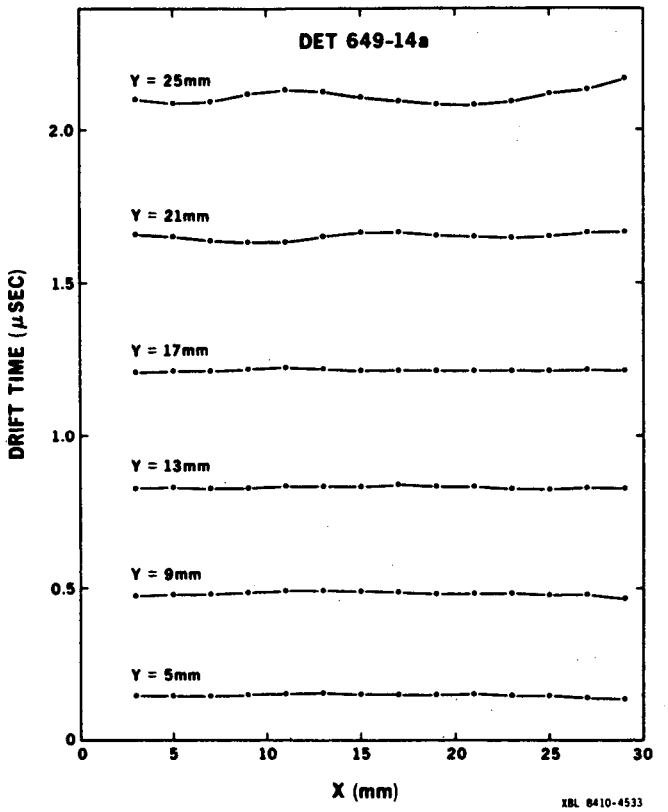

Fig. 9. Data taken from scans across the detector at various drift distances.

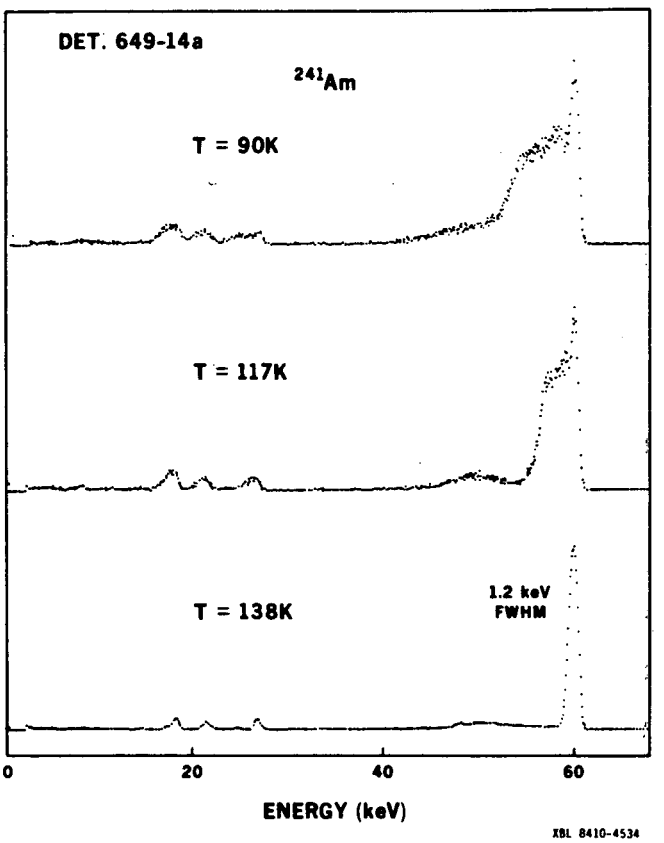

Fig. 10. Energy spectra of ^{241}Am taken by illuminating the full area of detector 649-14a at various temperatures. Amplifier peaking time = 4 μs.

twice that at 80 K, and that in actual operation, the detector must be maintained at a very stable temperature to avoid serious fluctuations of the drift time. For example, for this detector at 80 K and Y = 25 mm, a change of 1 degree (K) will shift the drift time by ~ 30 ns corresponding to ~ 0.3 mm in distance.

DLTS measurements of a crystal cut adjacent to detector 649-14a indeed showed the presence of electron traps characterized by a broad peak centered around 50 K at a concentration of ~ 1 x $10^9 cm^{-3}$ (Fig. 11a). These electron traps seem to be quite common and have been seen in high-purity germanium crystals grown at different facilities. The concentration of these traps has been correlated with the degradations in the energy resolutions of n-type reverse-electrode coaxial detectors by Hubbard, et al. [4]. The trapping effects are of course much amplified for the "drift chambers" because of the very low drift field.

Crystal 603 also showed similar electron traps (Fig. 11b) but at a lower concentration of ~ 3 x $10^8 cm^{-3}$. The origin of the two extra peaks seen in this spectrum is not known at the present time. The full area ^{241}Am spectrum obtained from 603-14a at ~ 80 K showed a much improved spectral shape compared to 649-14a (Fig. 12). This may be a combined result of lower trap concentration and higher transverse drift field. Unfortunately, this detector exhibits large non-uniformities in the drift times along both the X and Y directions (Fig. 13). The strongest variations occur near the center of the detector corresponding to the core of the original crystal. Abrupt increases of drift time occur at approximately Y = 11 mm and 19 mm which imply the existence of comparably smaller impurity gradients at those positions. At Y > 20 mm, no signal is observed around the center of the detector which indicates the presence of very small or even negative impurity gradients at that part of the crystal. This detector was made from a section of the crystal where the diameter changes rapidly which may be related to the large variations in the impurity gradient.

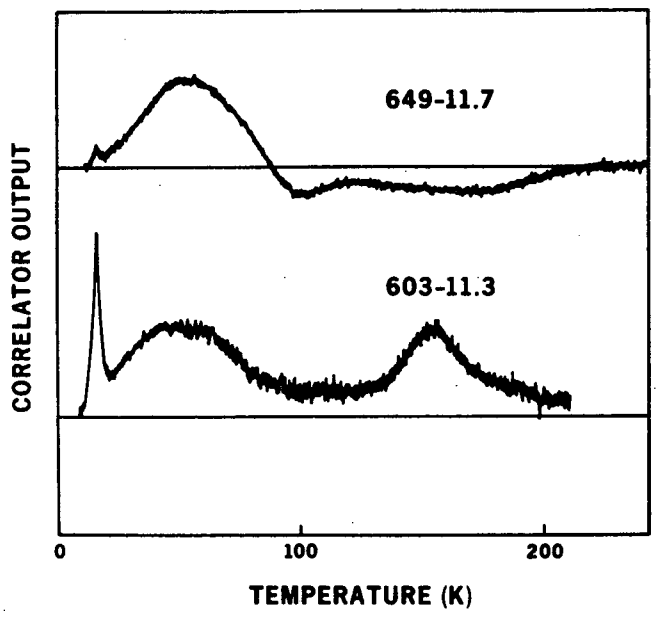

Fig. 11. DLTS spectra showing the presence of electron traps. Correlator time constant = 10 ms.

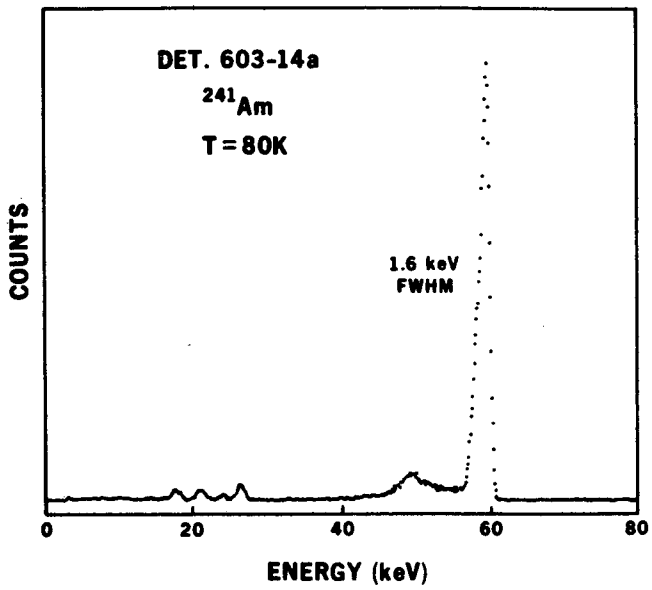

Fig. 12. Full area spectrum of ^{241}Am from detector 603-14a at ~ 80 K. Detector bias = 400 V.

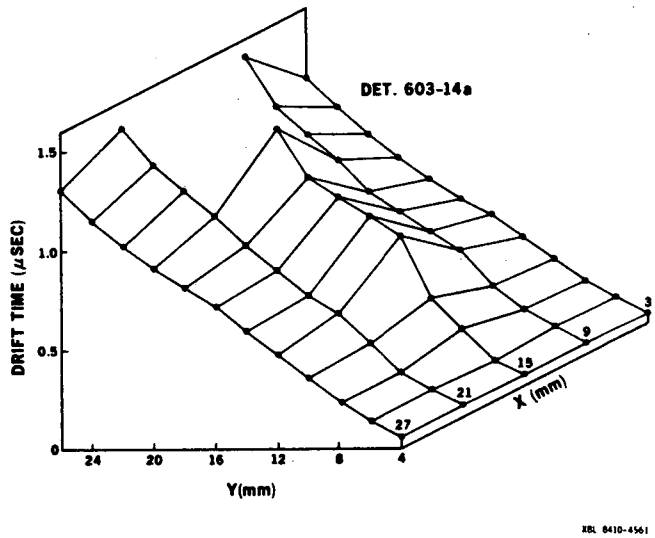

Fig. 13. Drift time versus position of detector 603-14a.

Conclusion

By using germanium crystals with an impurity concentration gradient, detectors with a built-in transverse drift field have been fabricated. The unique signals obtained from such detectors facilitate the measurement of carrier drift times and make possible the position determination of photons. One-dimensional spatial resolution $\lesssim$ 0.5 mm over an active area of ~ 2.5 x 2.5 cm^2 is realized in detector 649-14a for 60 keV photons. The simplicity of such a detector in terms of fabrication and in terms of the associated electronics and cryostat construction makes them attractive alternatives compared with conventional discrete element detectors.

The greatest limitations on such semiconductor "drift chambers" are the non-uniformity or non-linearity in the impurity distribution of the crystal, and the presence of electron traps. The first problem is related to the variations in the crystal growth conditions. The detectors reported here are fabricated from

"left-over" sections of germanium crystals that happen to exhibit the suitable impurity gradient. They are located near the tail end of the crystals where crystal growth conditions were changing rapidly. The situation may be more favorable if crystals were grown specifically for such detectors by intentional doping. For the present, we believe that the demonstration in detector 649-14a of good uniformity and linearity is an indication of great promise. Moreover, nonlinearities in the drift time can be easily corrected for by computer-stored calibrations.

The origin and identity of the electron traps are not well understood at the present time. However, since they also affect the performance of reverse-electrode coaxial detectors, efforts are being made toward understanding and controlling these defects [4]. As detector 603-14a showed, a trap concentration $\sim 10^{8}cm^{-3}$ may produce acceptably small degradation in energy resolution, at least for low energy gamma rays. In addition, the effects of trapping can be greatly reduced by slightly increasing the temperature of the detector.

Acknowledgements

We thank E. Gatti of Instituo di Fisica, Politecnico di Milano, Italy and P. Rehak of Brookhaven National Laboratory for interesting discussions which inspired this work originally. We are grateful to C. Cork, J. T. Felts, E. E. Haller, D. Malone and R. Pehl for their input and contributions to this work.

This work was supported by the Director's Office of Energy Research, Office of Health and Environmental Research, U.S. Department of Energy under Contract No. DE-AC03-76SF00098.

References

[1] E. Gatti and P. Rehak, presented at the 2nd Pisa Meeting on Advanced Detectors, Grosetto, Italy, June 3-7, 1983. Nucl. Instr. and Methods, vol. 225, No. 3, 608 (1984). BNL-33523.

[2] E. Gatti, P. Rehak and J. T. Walton, presented at the 3rd European Symposium on Semiconductor Detectors, Munich, Nov. 14-16, 1983. Nucl. Instr. and Methods, vol. 226, No. 1, 129 (1984). See also the paper presented in this conference.

[3] E. E. Haller, W. L. Hansen and F. S. Goulding, Advances in Physics, vol. 30, No. 1, 93 (1983).

[4] G. S. Hubbard, E. E. Haller and S. J. Pearton, presented at the 13th International Conference on Defects in Semiconductors, San Diego, Aug. 13-17, 1984. See also the paper presented in this conference.

This report was done with support from the Department of Energy. Any conclusions or opinions expressed in this report represent solely those of the author(s) and not necessarily those of The Regents of the University of California, the Lawrence Berkeley Laboratory or the Department of Energy.

Reference to a company or product name does not imply approval or recommendation of the product by the University of California or the U.S. Department of Energy to the exclusion of others that may be suitable.

TECHNICAL INFORMATION DEPARTMENT
LAWRENCE BERKELEY LABORATORY
UNIVERSITY OF CALIFORNIA
BERKELEY, CALIFORNIA 94720